

Multiple Features of Motor-Unit Activity Influence Force Fluctuations During Isometric Contractions

Anna M. Taylor, Evangelos A. Christou, and Roger M. Enoka

Department of Integrative Physiology, University of Colorado, Boulder, Colorado 80309-0354

Submitted 21 January 2003; accepted in final form 6 April 2003

Taylor, Anna M., Evangelos A. Christou, and Roger M. Enoka. Multiple features of motor-unit activity influence force fluctuations during isometric contractions. *J Neurophysiol* 90: 1350–1361, 2003. First published April 17, 2003; 10.1152/jn.00056.2003. To identify the mechanisms responsible for the fluctuations in force that occur during voluntary contractions, experimental measurements were compared with simulated forces in the time and frequency domains at contraction intensities that ranged from 2 to 98% of the maximum voluntary contraction (MVC). The abduction force exerted by the index finger due to an isometric contraction of the first dorsal interosseus muscle was measured in 10 young adults. Force was simulated with computer models of motor-unit recruitment and rate coding for a population of 120 motor units. The models varied recruitment and rate-coding properties of the motor units and the activation pattern of the motor-unit population. The main finding was that the experimental observations of a minimum in the coefficient of variation (CV) for force (1.7%) at approximately 30% MVC and a plateau at higher forces could not be replicated by any of the models. The model that increased the level of short-term synchrony with excitatory drive provided the closest fit to the experimentally observed relation between the CV for force and the mean force. In addition, the results for the synchronization model extended previous modeling efforts to show that the effect of synchronization is independent from that of discharge-rate variability. Most of the power in the force power spectra for the models was contained in the frequency bins below 5 Hz. Only a model that included a low-frequency oscillation in excitation, however, could approximate the experimental finding of peak power at a frequency below 2 Hz: 38% of total power at 0.99 Hz and 43% at 1.37 Hz, respectively. In contrast to the experimental power spectra, all model spectra included a second peak at a higher frequency. The secondary peak was less prominent in the synchronization model because of greater variability in discharge rate. These results indicate that the variation in force fluctuations across the entire operating range of the muscle cannot be explained by a single mechanism that influences the output of the motor-unit population.

INTRODUCTION

The force that a motor unit exerts depends on the rate at which the motor neuron discharges action potentials (Macefield et al. 1996; Thomas et al. 1991). When the discharge rate is less than that required for a fused tetanus, the force exerted by the motor unit will fluctuate about an average value. Because discharge rates during voluntary contractions rarely achieve tetanic rates (Enoka and Fuglevand 2001), the force exerted by a muscle will include fluctuations in force due

to the submaximal activation of many motor units. Furthermore, the amplitude of the force fluctuations increases as more motor units are recruited (Christou et al. 2002; Slifkin and Newell 1999; Yao et al. 2000).

The contribution of a motor unit to the fluctuations in force changes as a function of the contraction intensity. First, as the level of voluntary activation of the motor-neuron pool increases, so does the discharge rate of the activated motor neurons (Person and Kudina 1972), which reduces the fluctuations in motor-unit force. Second, the relative increment in whole muscle force attributed to the recruitment of a motor unit declines with an increase in contraction intensity (Fuglevand et al. 1993), which causes high-threshold motor units to contribute less to the force fluctuations. In contrast, the activation pattern of the motor-unit population can enhance the force contributed by a single motor unit. For example, increased levels of short-term synchronization, which appear to be caused by greater amounts of branched common input (Sears and Stagg 1976; Semmler 2002), increase motor-unit force and the fluctuations in whole muscle force (Taylor et al. 2002; Yao et al. 2000).

The purpose of this study was to identify those features of motor-unit activity that are responsible for the variation in force fluctuations across the operating range of the first dorsal interosseus muscle. This was accomplished by comparing experimental observations with computer simulations involving several models of motor-unit recruitment and rate coding (Fuglevand et al. 1993; Taylor et al. 2002). Each model involved manipulation of a single variable so that it was possible to examine the influence of recruitment range, the distribution of discharge rates, short-term synchronization, and oscillation in excitatory drive on the pattern of force fluctuations. The results indicate that variation in the force fluctuations during voluntary contractions that spanned the operating range of the muscle cannot be explained by a single mechanism that influences motor-unit activity. This finding contrasts with some experimental observations that the force fluctuations, particularly at low forces, are largely attributable to discharge-rate variability (Kornatz et al. 2002; Laidlaw et al. 2000; Patten and Kamen 2000).

METHODS

Ten young adults (5 men and 5 women) participated in the study. The mean \pm SD for the age of the subjects was 29.4 ± 4.4 yr, ranging

Address for reprint requests: R. M. Enoka, Department of Integrative Physiology, University of Colorado, Boulder, CO 80309-0354 (E-mail: roger.enoka@colorado.edu).

The costs of publication of this article were defrayed in part by the payment of page charges. The article must therefore be hereby marked "advertisement" in accordance with 18 U.S.C. Section 1734 solely to indicate this fact.

from 22 to 36 yr. All subjects were right-handed and had no known neurological disorders. The protocol was approved by the Human Subjects Committee at the University of Colorado and performed with the informed consent of the subjects.

Force measurement

Subjects sat facing a 17-in. computer monitor with the left arm abducted by 0.79 rad and the left hand resting prone on a platform. The monitor was 1.6 m in front of the subject at eye level. The height of the platform was adjusted so that the shoulders were horizontal. A vacuum foam pad was used to immobilize the elbow and forearm (Versaform pillow, Tumble Forms, Trenton, Ontario, Canada). The left hand and forearm were constrained by clamps to maintain an angle of 0.8 rad between the thumb and index finger (Fig. 1). The index finger was inserted into a splint that kept the interphalangeal joints extended.

The abduction force exerted by the index finger was measured with a force transducer (Model 13, Sensotec) that was aligned with the proximal interphalangeal joint. A high sensitivity (0.051 V/N) transducer was used for contractions that were <20% maximum voluntary contraction (MVC) force, and a low-sensitivity (0.0059 V/N) transducer was used to measure force during contractions that were \geq 20% MVC force. The signal-to-noise ratio for the force transducer at the lowest force (0.8 N) for the steadiest subject was 3.82, and averaged 11.5 ± 7.28 (range: 3.82–24.6) for all subjects at the minimum target force (2% MVC). Force was sampled at 500 Hz using Spike2 software (CED, Cambridge, UK) and stored on a computer.

A horizontal line was placed on the computer monitor to indicate the target force for each trial. The gain of the force display was adjusted so that the target-force line was always at the same location on the monitor. The task involved matching the target force within 1 s of trial initiation and then sustaining the abduction force for 6 s. Each subject received visual feedback of the target force and the force exerted by the index finger during the first 3 s of a contraction, after which the monitor was blocked from the subject's view for the remainder of the trial. Before the start of data collection, the subject was instructed not to flex, extend, or rotate the index finger during the contractions. Furthermore, the subject was informed that a trial would be terminated if one of the experimenters observed any index finger motion besides abduction. Positions of the index finger and arm were constantly monitored by one of the investigators during each trial. At

the conclusion of each trial, the force exerted during the entire contraction was displayed on the monitor for the subject to view.

EMG measurement

Electromyographic (EMG) activity of the first dorsal interosseus muscle was measured with silver–silver chloride electrodes (4-mm diameter) that were attached to the skin. One electrode was placed over the belly of the muscle (proximal one-third) and a second electrode was placed over the metacarpophalangeal joint (Zijdewind et al. 1999). The reference electrode was attached to the skin over the styloid process of the ulna. The EMG signals were amplified ($\times 1,000$) with an isolated bioamplifier (S-series, Coulbourn, Instruments, Allentown, PA), passed through a band-pass filter (20 to 800 Hz; S-series, Coulbourn Instruments), and sampled at 4 kHz (1401 plus, Cambridge Electronic Design, UK).

Experimental protocol

The protocol consisted of two 6-s contractions at each of 9 target forces. To determine the target forces, each subject first performed two or more MVCs until the peak forces for at least two of the MVCs were within 5% of each other. Performance during the MVCs was monitored for unwanted motion of the index finger. The peak force exerted during an acceptable MVC trial was taken as the MVC force (Allen et al. 1995). The 9 target forces corresponded to 2, 5, 15, 30, 50, 70, 85, 95, and 98% of MVC force. The order of the target forces was randomized for each subject. Adequate rest was given between trials to minimize fatigue—a minimum of 30 s or until the subject felt fully recovered from the previous trial. At the conclusion of the protocol, the subject performed another MVC for comparison with the value obtained at the beginning of the protocol.

Motor-unit model

A model of recruitment and rate coding (Fuglevand et al. 1993; Taylor et al. 2002; Yao et al. 2000) was used to simulate the isometric force produced by a pool of 120 motor units (Fig. 2). The model was implemented in Matlab version 6.1 (The Mathworks, Natick, MA). The basic parameters of the model were the same as those reported previously (Taylor et al. 2002) and were chosen to approximate the characteristics of the motor-unit population in the first dorsal interosseus (Enoka and Fuglevand 2001).

In brief, the peak twitch forces of motor units [range: 1–100 arbitrary units (au)] were proportional to the recruitment threshold (range: 1–12 au) and were distributed exponentially across the population of 120 units. Because previous simulations (Enoka et al. 2003) suggested that a reduction in the number of motor units in the population by 25% and an increase in the range of twitch forces across the population by 40% had little effect on force fluctuations, these values were kept constant in the current simulations. The twitch contraction time of each motor unit in the model was inversely proportional to peak twitch force (range: 30–90 ms), and the force–frequency relation for each motor unit depended on its peak twitch force and contraction time.

Excitation of the motor-unit pool was modeled as a ramp-and-hold function, with a 1-s ramp increase in excitation to the mean level that was held constant for the remaining 4 s of simulated force (Fig. 2, B–E). In some trials, a sinusoidal excitation function was superimposed on the constant excitation from 1 to 4 s to simulate the rhythmic drive of the motor-unit pool. The amplitude of the oscillating drive was a fixed percentage of the mean excitation for that trial.

Variability in discharge rate was manipulated by multiplying the instantaneous discharge frequency produced in response to the excitation function by a random value with a Gaussian distribution and a coefficient of variation (CV) of 10%. Although this value is lower than that used in previous versions of the model (20%), the results

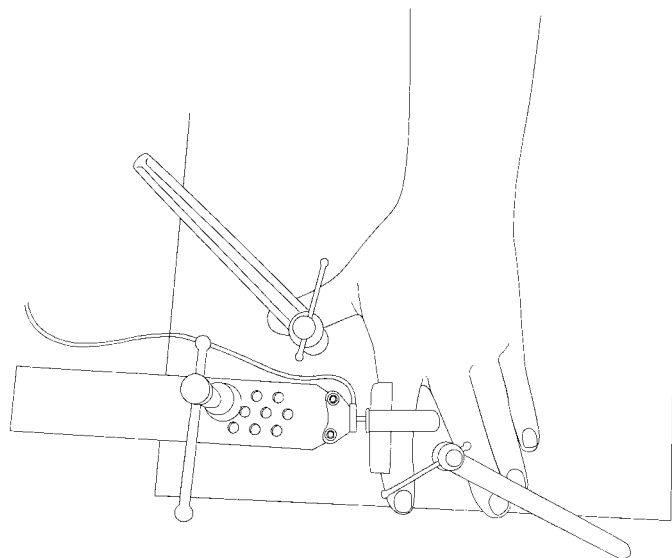


FIG. 1. Experimental setup. Subject's hand was flat on a platform and arm was placed in form-fitting vacuum pillow. Hand was prone and position of hand and fingers was held stationary with clamps. Index finger was placed in splint to prevent flexion at interphalangeal joints.

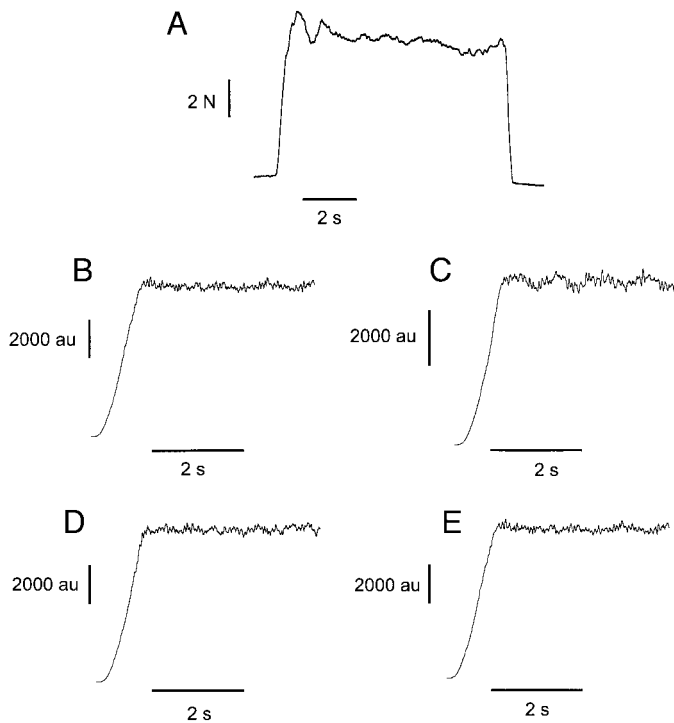


FIG. 2. Examples of isometric force at approximately 50% of maximum voluntary contraction for experimental data (A), basic model (B), 1-Hz oscillation model with an amplitude of 2% of mean excitation (C), 20-Hz oscillation model with amplitude of 10% of mean excitation (D), and synchronization model (E).

obtained with a CV of 10% more closely approximated the experimentally measured force variability. All motor units had a minimum discharge rate of 8 Hz, but peak discharge rate declined linearly with recruitment threshold. Discharge rates increased linearly with increased excitation. Once each model motor unit reached its assigned maximal rate, the rate was fixed despite any further increases in excitation. The first recruited unit (motor unit 1) had a maximal discharge rate of 35 Hz, whereas the peak value for motor unit 120 was 25 Hz.

Whole muscle force was simulated as the linear sum of the single motor-unit forces. The force contributed by each motor unit was derived as the impulse response each time an action potential was discharged by the motor neuron (Fuglevand et al. 1993).

The parameters of the basic model were adjusted to examine the influence of the pattern of excitation, recruitment range, and rate coding on the fluctuations in the simulated force. Only one parameter was adjusted in each simulation. The following parameters were varied and the results were compared with the basic model: 1) gain—the increase in instantaneous discharge rate with an increase in excitation was varied from one (basic model) to two; 2) nonuniform gain—a variation in gain between values of 2.0 and 0.75 across the motor-unit pool, which changed either proportionally or inversely with recruitment threshold; 3) minimum discharge rate—4 and 10 Hz compared with 8 Hz in the basic model; 4) peak discharge rate—a 10-Hz increase in the peak discharge rate for all motor units; 5) range of peak discharge rates—a 20-Hz decline in peak discharge rate between motor unit 1 (35 Hz) and motor unit 120 (15 Hz), compared with a 10-Hz decrease in the basic model; 6) distribution of peak discharge rates—a higher discharge rate for motor unit 120 compared with motor unit 1, which was tested for each of the ranges and values of peak rates; 7) coefficient of variation for discharge rate—10 and 20%; 8) recruitment range—a recruitment threshold range of 54 and 69% compared with 41% of maximal excitation for the basic model; 9) oscillating activation—at frequencies of 1, 8, 10, 12, and 20 Hz

with amplitudes of 2, 5, 10, and 20% of mean excitatory drive; and 10) motor-unit synchronization—a linear increase with excitation compared with no synchrony in the basic model.

A number of the changes to these 10 parameters either had no effect on the force fluctuations or greatly altered the magnitude and pattern of the force produced by the model. To simplify the comparisons in the present study, only the parameters that had a direct effect on the force fluctuations were analyzed further. Only 5 variations of the parameters listed above met this criterion and were compared with the basic model: 1) recruitment range of 69%; 2) motor-unit synchronization; 3) oscillating activation of 1 Hz at 2% of mean excitation, 12 Hz at 10%, and 20 Hz at 10%; 4) peak discharge rate increase by 10 Hz for all motor units; 5) range of peak discharge rates with motor unit 120 discharging at a 20-Hz lower peak rate than that of motor unit 1. Similar to the experimental trials, 10 simulations were run at each of 10 force levels (2, 5, 15, 30, 50, 70, 85, 95, 98, and 100% of maximal force) and force was sampled at 500 Hz.

As with the experimental trials, the simulated forces were quantified as a percentage of maximal force. Because the force–excitation relation depended on the parameters used in the model, the level of excitation required to simulate the target force was determined from polynomial functions that were fitted to the forces obtained with 10 simulations at each of 10 levels of excitation for the different models (Fig. 3).

Because the distribution of discharge times has a significant effect on force variability (Enoka et al. 2003; Taylor et al. 2002), the mean discharge rate and CV for discharge rate were kept the same, except for the condition that involved an explicit comparison of the effect of discharge-rate variability. The only condition in which this was not possible was the synchronization condition. In this case, the mean rate was the same as the other models across the different levels of excitation, but the variability increased from 16.4 to 32% as the level of excitation increased from a minimum to maximum; for comparison, the CV for discharge rate increased from 10 to 15.6% in the basic model. The consequences of this difference in variability are addressed in the DISCUSSION.

Synchronization was applied by adjusting some of the discharge times of each motor unit to be approximately coincidental with the discharges of other motor units. These methods were previously presented in detail (Taylor et al. 2002). In the present simulations, synchronization progressed linearly from low to high with increased

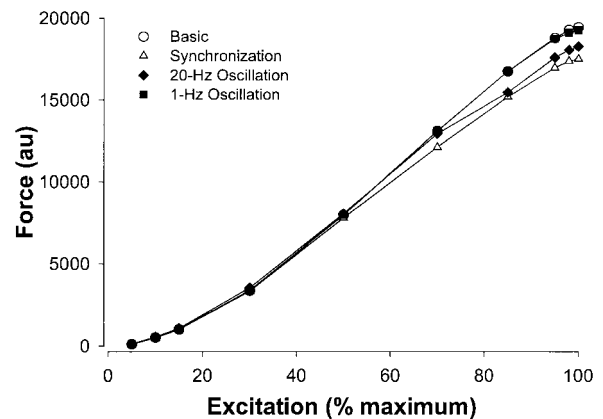


FIG. 3. Force–excitation relations for models were all nonlinear. To obtain forces at similar percentages of maximal force, excitation values for simulation trials were predicted from individual force–excitation functions of models. Functions used to predict force (y) based on excitation (x) were: $y = 5.6 + 6.5x + 4.2x^2 - 0.023x^3$ for basic model, $y = -236.9 + 45.2x + 3.4x^2 - 0.020x^3$ for 20-Hz oscillation model, $y = -205.5 + 36.9x + 3.4x^2 - 0.020x^3$ for synchronization model, and $y = 38.9 + 2.4x + 4.4x^2 - 0.024x^3$ for 1-Hz oscillation model.

excitation. The number of discharge adjustments was defined by

$$S = \frac{0.25}{E_{\text{Max}}} E_i$$

where S is the percentage of the reference units that were adjusted, E_{Max} is the excitation applied for maximal force, and E_i is the excitation required for the force-matching trial. Motor-unit synchronization for the population was quantified by obtaining indexes of synchronization [common input strength (CIS) index and E index] for every tenth recruited motor unit with the 15 preceding and the 15 succeeding motor units; the number of succeeding units, however, was limited to those recruited during the trial. The CIS index indicates the frequency of extra synchronous discharges, whereas the E index denotes the probability of extra synchronous discharges for every discharge by the reference motor unit. The average level of motor-unit synchronization increased from 0.17 to 2.20 impulses/s (CIS index) and from 0.020 to 0.072 impulses/trigger (E index) as the simulated force increased from 2 to 98% of MVC.

Data analysis

All data analysis was performed with custom-written programs in Matlab version 6.1 (The Mathworks). Analyses were performed separately for the visual (first 3 s) and nonvisual (last 3 s) parts of each target-matching trial. For the nonvisual portion of each trial, 2 s of data were used beginning 500 ms after visual feedback was removed. After the force data were detrended, the SD of force and CV for force ($CV = SD/\text{mean}$) were calculated. The same analysis was completed between 1 to 3 s for the visual portions of each trial and for the simulation data. The EMG data were analyzed over these same intervals of time.

A frequency analysis was performed on the force (experimental and simulated) and EMG using a modified Welch's periodogram method with a Hanning window (no overlap) that had the same length as the FFT block size (512 points). The mean force was subtracted from each signal during the analysis. The resolution of the power spectra was 0.976 Hz for force and 8.04 Hz for the interference EMG. The analyses determined the percentage of total power in each frequency bin, the maximal power, the frequency at maximal power, and the median frequency.

Statistical analysis

All statistics were performed on the single trial that most closely matched the target force. One subject had no reasonable data for the 70% target force. A 2-factor, repeated-measures analysis of variance (ANOVA) (2 levels of vision \times 9 target forces) was used to compare the force variability during the visual and nonvisual conditions at the various target forces. Because the model did not include visual feedback, the statistical comparisons between the experimental and simulated data were made with the forces measured when the subjects did not have visual feedback.

A 2-factor, repeated-measures ANOVA was used to compare the experimental and simulated coefficients of variation for force (2 between-subject factors) across the 9 target forces (repeated-measure factor). Because there were 8 different model conditions (including 3 levels of oscillating drive), the number of comparisons was limited by selecting those models that matched the experimental data at 4 or more force levels. The alpha level for all statistical tests was $P \leq 0.05$. Significant interactions were followed by post hoc analyses (independent or dependent t -test with Bonferroni corrections).

Two-factor, repeated-measures ANOVAs were also used to compare the median frequency of the force and EMG power spectra. Stepwise regression analysis was used to detect significant linear associations between force fluctuations (SD and CV for force) and power at each frequency bin of the force signal (1–12 Hz of the

experimental data and 1–35 Hz of the model data). Similar regression analyses were used to examine the associations between the force fluctuations and the EMG power spectrum, and the power spectra for EMG and force.

RESULTS

This study involved a comparison of the forces exerted by a hand muscle during steady-state voluntary contractions with those simulated by several models of motor-unit recruitment and rate coding. The purpose was to identify those features of motor-unit activity that are responsible for the variation in force fluctuations across the operating range of the muscle.

Experimental measurements

Because of the progressive enhancement of motor-unit activity during the voluntary contractions, the amplitude of the interference EMG (y) increased linearly with target force (x) for all subjects ($y = 0.0147x + 0.1309$; $r^2 = 0.77$). The mean force, SD of force, and CV for force were similar for the visual and nonvisual parts of each voluntary contraction ($P > 0.05$). Although the force fluctuations during visual feedback tended to be of greater magnitude, the pattern across target forces was similar to that observed during the absence of the visual feedback. The fluctuations during visual feedback had a mean CV of $4.2 \pm 2.2\%$ at 2% MVC, which decreased to $1.7 \pm 0.78\%$ at 30% MVC and then increased again to $2.3 \pm 1.0\%$ at 98% MVC. The remainder of this report, however, focuses on the fluctuations during the absence of visual feedback for comparison with the simulated forces. The SD of force increased ($P < 0.05$) nonlinearly with target force (Fig. 4A; Table 1). Furthermore, the CV for force declined from a maximum at 2% MVC to a minimum at 30% MVC ($P < 0.05$), after which it increased to a plateau that began at 50% MVC (Fig. 4B; Table 1). These results did not appear to be influenced by fatigue, given that the MVC forces were similar ($P > 0.1$) at the beginning (25.7 ± 7.3 N; range: 18.3–36.0 N) and end of the protocol (26.6 ± 5.8 N; range: 19.4–34.0 N).

Maximal power in the force spectra during the experimental measurements (Fig. 5) occurred at low frequencies (1.37 ± 1.07 Hz; range: 0.98–6.08 Hz). On average, $42.8 \pm 5.8\%$ of the total power in the force signal was contained in the frequency bin corresponding to the maximal power. The median frequency in the force spectra tended to decrease as excitation increased, declining from 1.47 ± 1.8 Hz at the target force of 2% MVC to 0.22 ± 0.43 Hz at the target force of 70% MVC.

Maximal power in the interference EMG spectra (not shown) occurred at higher frequencies (68.4 ± 23.2 Hz; range: 32.2–145 Hz). On average only $8.71 \pm 2.79\%$ of the total power in the EMG signal was contained in the frequency bin where maximal power was located, which indicates that the power was distributed more broadly in the EMG spectrum than in the force spectrum. The median frequency of the EMG tended to decrease (range: 93.8–69.7 Hz) with target force; however, this decrease did not reach statistical significance ($P = 0.06$ for 5% compared with 98% MVC).

There was a significant positive association between the percentage of total power at 0.98 Hz in the force spectrum and the SD of force ($r^2 = 0.12$, $P < 0.01$). Similarly, the 0.98 and 9.8 Hz frequencies of the force power spectra were significantly related to the CV for force ($r^2 = 0.21$ and 0.01 ; $P <$

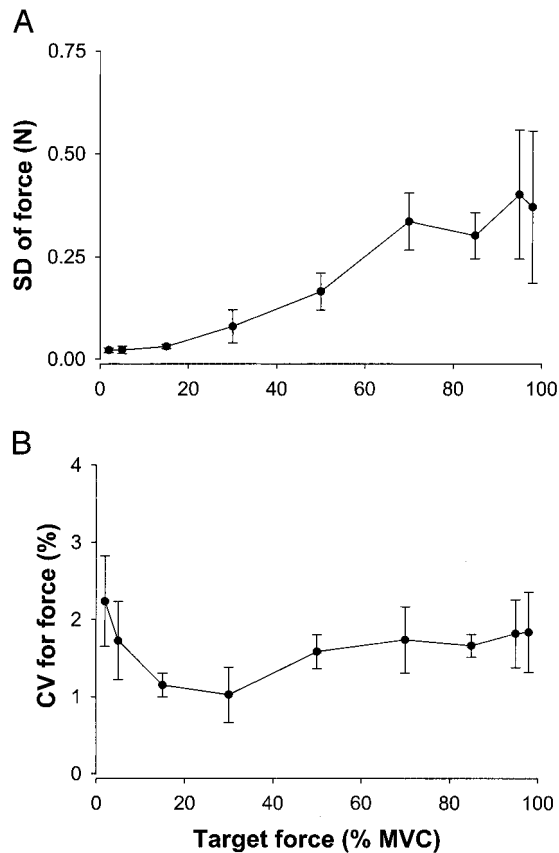


FIG. 4. Fluctuations in index finger force during voluntary contractions performed with first dorsal interosseus muscle. Data consist of those parts of each trial when subjects received no visual feedback. *A*: SD of force increased exponentially up to about 70% MVC force and then remained relatively constant. *B*: coefficient of variation (CV) for force was greatest at low forces, decreased to a minimum at 30% MVC, and then increased to plateau after 50% MVC. Data in *A* and *B* are plotted as median \pm SE for 10 subjects.

0.01, respectively). There was also a significant positive relation between the SD of force and the total power in the interference EMG signal from 50 to 75 Hz ($r^2 = 0.16$, $P <$

0.01); however, there was no significant association between the CV for force and the EMG power spectrum ($P > 0.05$). There were also some significant associations between the force and interference EMG spectra. For example, the power at 0.98 Hz in the force signal was negatively associated with the percentage total power in the EMG signal from 200 to 225 Hz ($r^2 = 0.09$, $P < 0.01$), whereas the power in the force spectrum between 4.8 and 6.8 Hz was positively correlated with the EMG power between 125 and 150 Hz ($r^2 = 0.09$, $P < 0.01$). Furthermore, the power at 8.8 Hz of the force signal was positively associated with the EMG power spectra in the range 225–250 Hz ($r^2 = 0.06$, $P < 0.05$).

Simulated forces

The various models used in the study had obvious effects on the discharge times of the motor units. These effects are characterized in raster plots for three of the models: basic, 1-Hz oscillation, and synchronization models (Fig. 6). The raster plots show the discharge times of selected motor units during a 3-s interval when the model was being excited to exert a force of 30% MVC. Compared with the basic model, there are marked changes in the discharge times for the other two models. For example, the oscillations are apparent in the discharge times for the 1-Hz oscillation model and the discharge times are much more variable for the synchronization model.

None of the motor-unit models was able to simulate the observed patterns of fluctuations in force (SD and CV for force) across the operating range of the muscle. Four models, however, approximated the experimentally measured coefficients of variation for force at 4 or more levels of force (Fig. 7B). The two most accurate models were the basic model and the model with an excitatory drive that fluctuated at 20 Hz (20-Hz oscillation), which had simulated CVs for force that were similar to the experimental measures at 2, 5, 50, 70, 85, 95, and 98% MVC. The synchronization model approximated the experimental CVs for force at 2, 5, 95, and 98% MVC. The fourth successful model, which included an excitatory drive that oscillated at 1 Hz (1-Hz oscillation), matched the experi-

TABLE 1. Experimental measures of the normalized force, absolute mean force, standard deviation of force, and coefficient of variation for force at nine target forces

Target Force	Force, % MVC	Force, N	Standard deviation, N	Coefficient of variation, %
2% MVC	3.8 \pm 0.81 (2.6–5.4)	0.93 \pm 0.20 (0.65–1.27)	0.026 \pm 0.018 (0.005–0.060)	2.7 \pm 1.9 (0.57–6.6)
5% MVC	5.3 \pm 0.85 (4.6–7.6)	1.3 \pm 0.31 (0.98–1.8)	0.032 \pm 0.028 (0.018–0.10)	2.3 \pm 1.6 (1.1–6.3)
15% MVC	10.7 \pm 1.7 (9.5–15.0)	2.7 \pm 0.58 (1.8–3.4)	0.033 \pm 0.016 (0.014–0.065)	1.2 \pm 0.49 (0.51–1.9)
30% MVC	30.9 \pm 1.6 (28.5–33.8)	7.9 \pm 2.3 (5.2–11.1)	0.12 \pm 0.12 (0.027–0.47)	1.4 \pm 1.1 (0.47–4.4)
50% MVC	50.9 \pm 1.5 (46.7–52.3)	12.9 \pm 3.8 (8.6–18.2)	0.22 \pm 0.14 (0.075–0.50)	1.59 \pm 0.70 (0.78–2.7)
70% MVC	68.3 \pm 4.0 (62.5–75.0)	18.0 \pm 5.3 (12.0–25.5)	0.36 \pm 0.22 (0.068–0.78)	2.0 \pm 1.3 (0.57–4.4)
85% MVC	83.3 \pm 4.2 (76.8–90.0)	21.5 \pm 6.3 (14.1–29.5)	0.35 \pm 0.18 (0.10–0.62)	1.55 \pm 0.47 (0.65–2.2)
95% MVC	92.0 \pm 5.2 (81.6–100.0)	23.7 \pm 6.9 (15.9–32.7)	0.55 \pm 0.50 (0.19–1.9)	2.2 \pm 1.4 (1.0–5.7)
98% MVC	97.3 \pm 3.3 (92.2–102.0)	24.9 \pm 7.0 (18.5–34.9)	0.64 \pm 0.58 (0.22–2.1)	2.4 \pm 1.6 (1.0–6.3)

Values are mean \pm SD (range).

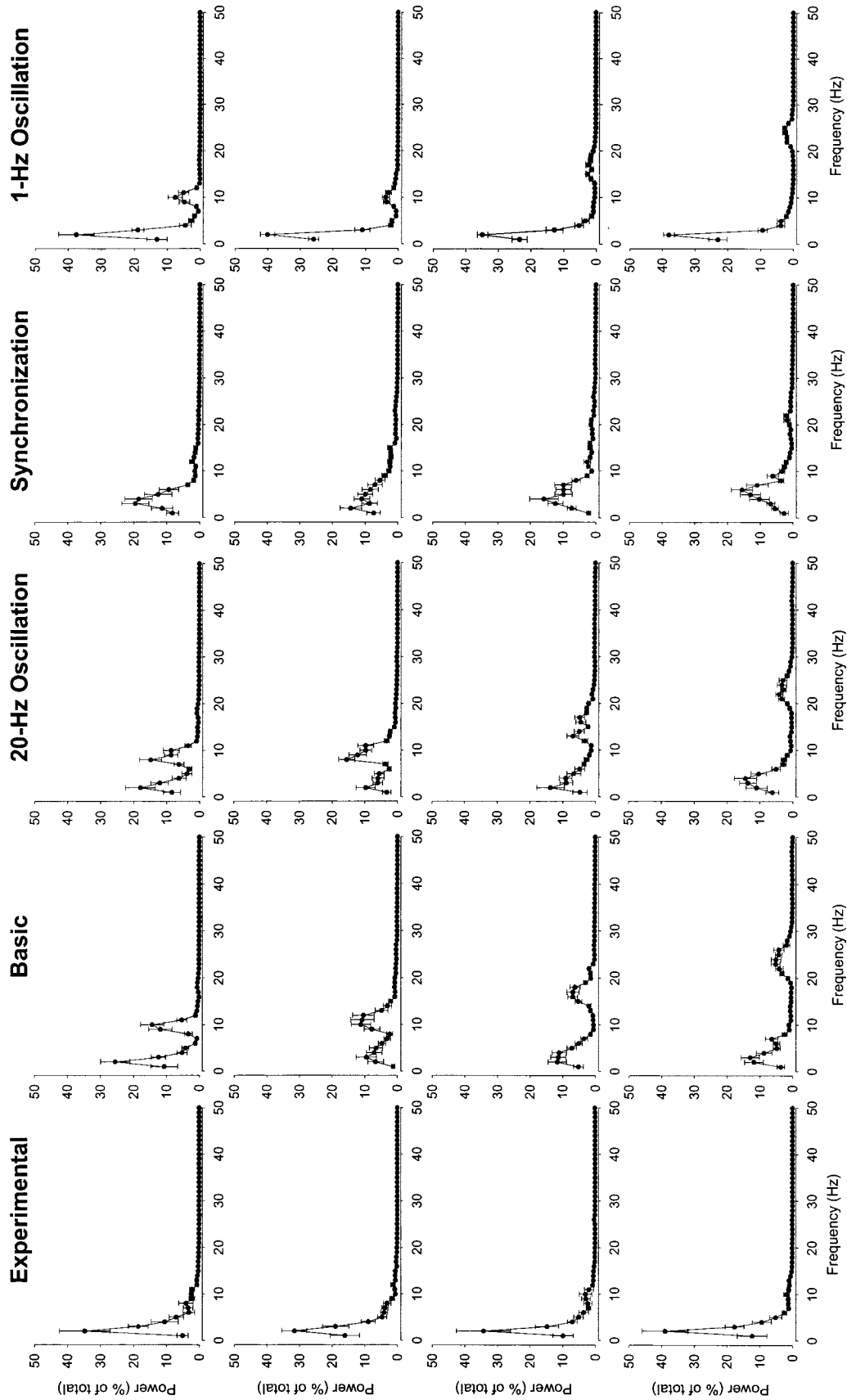


FIG. 5. Power spectra for experimentally measured force and force simulated with 4 models. Four rows (top to bottom) correspond to forces at 2, 15, 50, and 85% of MVC, respectively. Ordinate indicates percentage of total power contained in each frequency bin. Each power spectrum is mean \pm SE for 10 subjects or trials.

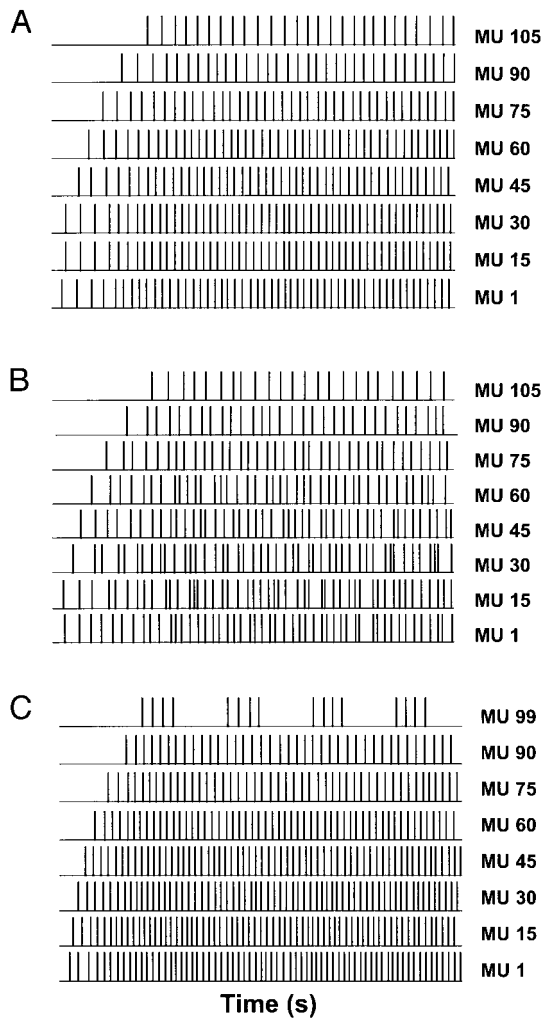


FIG. 6. Raster plots of simulated discharge times. Individual action potentials are represented as TTL-pulses for basic (A), synchronization (B), and 1-Hz oscillation (C) models for 0 to 3 s of the simulated contractions at 30% MVC. A: basic model had CV for discharge rate of 13.0% at this force level. B: increased number of coincident discharges is evident in raster plots for synchronization model, which had a CV for discharge of 32.5% for this trial. C: effect of excitation function for 1-Hz oscillation model can be seen with transient recruitment of highest threshold motor unit (motor unit 99) activated for this force level. CV for discharge rate for this trial was 12.6%.

mental coefficients of variation for force at 2, 5, 70, 95, and 98% MVC.

The models that could not approximate the experimental CVs for force at a minimum of 4 force levels had greater CVs for force than the experimental data (Fig. 7C). Thus they could match only the experimental force variability at high forces. The model with a 20-fold range in recruitment values could approximate the experimental force only at 70, 95, and 98% of MVC and the model that involved the 12-Hz oscillation could achieve a match only at 95 and 98% of MVC. Neither an increase in the peak discharge rate of motor unit 1 nor an increase in the difference between the peak discharge rates of motor units 1 and 120 could approximate the experimental force variation at any force level.

The frequency content of the simulated forces varied for the 4 models that matched the experimental measurements (Fig. 5). For example, although the median frequency generally increased with target force, the increase was from 3.4 to 7.9 Hz

in the basic model, from 3.02 to 6.64 Hz in the 20-Hz oscillation model, and from 1.66 to 4.59 Hz in the synchronization model. In contrast to the other models and similar to the experimental findings, the median frequency in the force spectra for the 1-Hz oscillation model decreased with force (0.98–0.10 Hz). Furthermore, only the 1-Hz oscillation model reproduced the average frequency at which the maximal power occurred (0.99 ± 0.53 Hz) and percentage of total power at that frequency ($37.5 \pm 2.25\%$) as observed experimentally (1.37 ± 1.07 Hz and $42.8 \pm 5.8\%$, respectively). The other three models exhibited higher frequencies of maximal power (basic: 5.11 ± 5.54 Hz; 20-Hz oscillation: 5.16 ± 5.32 Hz; and synchronization: 3.6 ± 1.71 Hz) and lower percentage of total power at that frequency (basic: $23 \pm 4.24\%$; 20-Hz oscillation: $23.3 \pm 2.7\%$; and synchronization: $24.2 \pm 4.4\%$) compared with the experimental data.

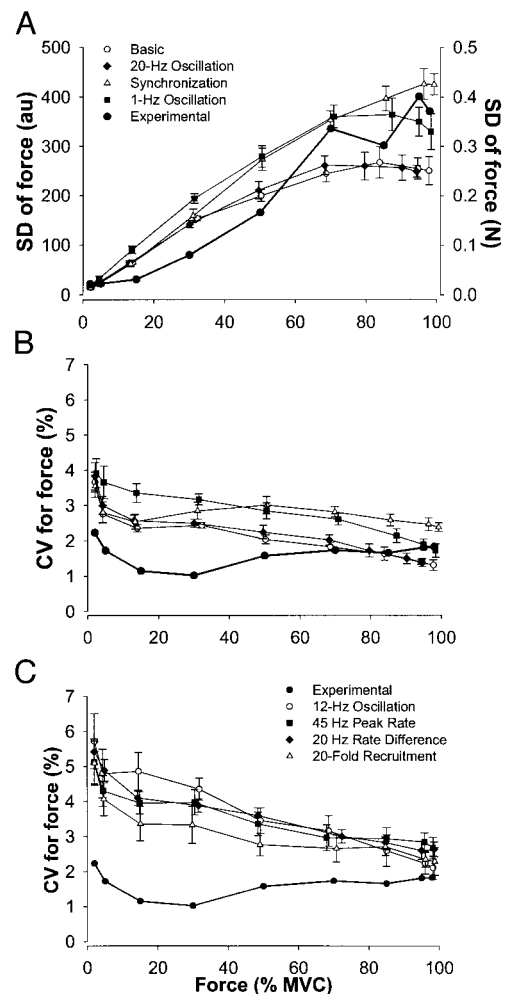


FIG. 7. SD and CV for force for simulated forces. A and B are for the models that could approximate data, whereas C shows data for 4 models that could not. A: SD of force increased more rapidly at low forces for simulated force compared with experimentally measured force. However, SDs of both experimental forces (right ordinate) and simulated forces reached a plateau at high forces. B: CV for force was initially greater than experimental values for all models and, with exception of synchronization model, simulated forces all decreased with increases in target force. C: CV for models that did not match experimental data were initially very high and decreased toward experimental values at high forces. Data for each model are plotted in arbitrary units (au) as mean \pm SE of 10 trials at each force. Experimental data are redrawn from Fig. 3.

TABLE 2. Associations between standard deviation of force and selected frequencies in the force power spectra for four models

Basic ($r^2 = 0.69, P < 0.001$)		20-Hz Oscillation ($r^2 = 0.57, P < 0.001$)		Synchronization ($r^2 = 0.51, P < 0.001$)		1-Hz Oscillation ($r^2 = 0.70, P < 0.001$)	
Frequency, Hz	Correlation Coefficient	Frequency, Hz	Correlation Coefficient	Frequency, Hz	Correlation Coefficient	Frequency, Hz	Correlation Coefficient
8.8	-0.639	8.8	-0.309	5.9	0.252	0.98	-0.008
9.8	-0.520	15.6	0.274	7.8	0.352	7.8	-0.553
18.6	0.297	22.5	0.458	28.3	0.323	9.8	-0.638
20.5	0.424	27.3	0.443	30.3	0.380	21.5	0.436
23.4	0.511	35.2	0.561	34.2	0.287	24.4	0.454
25.4	0.440						
35.2	0.369						

The reported frequencies contributed significantly ($P < 0.05$) to the SD of the simulated forces, as determined with a stepwise regression model. The r^2 values represent the fit of each regression model (5–7 frequencies) to the SD of the simulated forces.

Furthermore, three of the successful models (basic, 20-Hz oscillation, and 1-Hz oscillation) exhibited a distinct secondary peak in the force spectrum (Fig. 5). The frequency at which the secondary peak occurred increased with excitation, in parallel with the change in the mean discharge rate. For example, the basic model exhibited a second peak in the power spectrum that progressed from approximately 9 to 24 Hz as the target force increased from 2 to 85% MVC. In contrast, the power in the force spectra for the experimental data and the synchronization model was largely contained within a single range of low frequencies.

For these 4 models, the power in various frequencies of the force spectrum was significantly associated with the SD (Table 2) and CV for force (Table 3). With the exception of the synchronization model, the SD of force increased when there was more power at higher frequencies (>15 Hz) and less power at lower frequencies (<10 Hz) (Table 2). In contrast, the CV for force increased when there was greater power at lower frequencies (<10 Hz) and less power at higher frequencies (>20 Hz) (Table 3). These associations between the simulated force spectra and the SD and CV for force are contrary to those observed for the experimental data.

DISCUSSION

Much of the experimental evidence on the origin of force fluctuations during isometric contractions has focused on isolating a single explanatory mechanism. Among the candidate

mechanisms, the CV for motor-unit discharge rate has thus far seemed to be the most likely factor. Discrepancies in the literature, however, suggest that variability in discharge rate cannot account for the magnitude of the force fluctuations exhibited by all groups of subjects at all contraction intensities. Therefore this study examined several mechanisms hypothesized to influence the fluctuations in force during voluntary contractions with the first dorsal interosseus muscle across its entire operating range. This was accomplished by comparing the characteristics of experimentally measured forces with those obtained by computer simulation using models of motor-unit recruitment and rate coding.

The findings of this study extended previous investigations of force variability exhibited by the first dorsal interosseus by quantifying the time- and frequency-domain characteristics of force and EMG across a large range of isometric forces (2–98% of MVC). The results indicate that the relation between the CV for force and mean force can be characterized by a cubic polynomial, which differs from the hyperbolic relation observed at low forces (Enoka et al. 2003; Jones et al. 2002). The simulations confirm that discharge characteristics of the motor-unit population, such as synchronization and low-frequency common oscillation, are likely contributors to the observed time- and frequency-domain features of the force signal. Disparities between the simulations and the experimental observations, however, suggest that multiple mechanisms contribute to force variability across the operating range of the muscle.

TABLE 3. Associations between coefficient of variation for force and selected frequencies in the force power spectra for four models

Basic ($r^2 = 0.69, P < 0.001$)		20-Hz Oscillation ($r^2 = 0.62, P < 0.001$)		Synchronization ($r^2 = 0.26, P < 0.001$)		1-Hz Oscillation ($r^2 = 0.73, P < 0.001$)	
Frequency, Hz	Correlation Coefficient	Frequency, Hz	Correlation Coefficient	Frequency, Hz	Correlation Coefficient	Frequency, Hz	Correlation Coefficient
0.98	0.225	0.98	0.025	2.0	0.346	0.98	0.113
7.8	0.483	8.8	0.393	25.4	-0.296	7.8	0.430
8.8	0.563	22.5	-0.488	34.2	-0.325	9.8	0.566
22.5	-0.404	27.3	-0.511			23.4	-0.528
28.3	-0.559	29.3	-0.490			27.3	-0.467
30.3	-0.415	34.2	-0.412			29.3	-0.482
33.2	-0.424					32.2	-0.326

The reported frequencies contributed significantly ($P < 0.05$) to the CV for the simulated forces, as determined with a stepwise regression model. The r^2 values represent the fit of each regression model (3–7 frequencies) to the CV for the simulated forces.

Experimental data

Previous studies that quantified the variability in the abduction force exerted by the index finger during isometric contractions with the first dorsal interosseus muscle included no more than 5 force levels up to maximal contraction strengths of 75% MVC force. In studies that included forces $\leq 30\%$ MVC, the CV for force generally decreased as the mean force increased (Laidlaw et al. 1999, 2000). In one study that included forces $\leq 75\%$ MVC, however, the CV for force declined to 20% MVC and increased at 50 and 75% MVC (Burnett et al. 2000). Furthermore, the results obtained with previous simulations (Enoka et al. 2003; Jones et al. 2002), which predicted the pattern of force variability at higher forces, also showed a hyperbolic decline in CV for force as the mean level of force increased.

In contrast, the data included in the current report were obtained from a greater range of excitation levels and demonstrate a different relation between the CV for force and the mean force. The relation constituted an initial decrease in the CV for force to a minimum around 30% MVC force followed by an increase to a plateau that began at 50% MVC force. These results are consistent with those observed in other muscles, such as quadriceps femoris (Christou et al. 2002). The similarity of the relation for such different muscle groups, combined with the absence of an effect of visual feedback on the change in the amplitude of the force fluctuations, suggests that it may be a consequence of the activation signal sent to muscles during isometric contractions. Because of the nonlinear effects of summing motor-unit potentials on the time- and frequency-domain characteristics of the EMG signal (Day and Hulliger 2001; Fuglevand et al. 1993), however, there were only weak ($r^2 = 0.0083 \pm 0.0015$), although statistically significant, associations between the force fluctuations and the EMG. Consequently, the potential contributions of various activation strategies were examined with models of motor-unit recruitment and rate coding.

Mechanisms responsible for force variability

Three categories of mechanisms could influence the motor output from a population of motor units: 1) organization of the motor-unit pool; 2) recruitment and rate-coding properties of the motor units; and 3) the activation pattern of the motor-unit population. Organization of the motor-unit pool includes the number of motor units in the muscle and the twitch force properties of those motor units. Because the force contributed by a single motor unit to the net muscle force declines as the number of active motor units increases (Fuglevand et al. 1993), a muscle with fewer motor units might exhibit greater force fluctuations. Similarly, briefer twitches are associated with less fusion in motor-unit force at a given activation rate, which causes greater force variability, at submaximal levels of excitation. Findings from training programs (Keen et al. 1994; Kornatz et al. 2002; Laidlaw et al. 1999) suggest, however, that reorganization of the motor-unit pool is not a significant contributor to force variability. For example, the magnitude of fluctuations in the abduction force exerted by the index finger decreased during the first 4 wk of strength training without altering either the amplitude or the time course of the spike-triggered average twitch forces (Keen et al. 1994). Furthermore, simulation studies indicate that a 25% reduction in the

number of motor units and a 40% increase in the range of twitch forces for a population of motor units does not significantly influence the CV for force (Enoka et al. 2003; Taylor et al. 2000). This magnitude of reduction was used to approximate the loss that could be expected during healthy aging in humans.

The recruitment and rate-coding properties of the motor-unit pool, which constitute the second category of mechanisms, correspond to the discharge characteristics of the motor units with variation in the level of excitation. This includes such characteristics as the range of motor-unit recruitment, the discharge rates of the motor units in the population, and the variability of discharge rate at a given level of excitation. Motor-unit recruitment and discharge-rate modulation influence force by altering the amount of twitch fusion. Previous simulations have demonstrated that variation in the CV for discharge rate can cause pronounced changes in the force fluctuations (Enoka et al. 2003; Taylor et al. 2000). Consistent with this effect, experimental measurements have demonstrated significant associations between the CVs for the discharge rate of motor units in the first dorsal interosseus and the abduction force exerted by the index finger (Kornatz et al. 2002; Laidlaw et al. 2000). There have been exceptions to this observation, however, given that Semmler et al. (2000) found greater variability in index finger force between young and old adults, but no difference in the CV for discharge rate. Furthermore, Patten and Kamen (2000) found that a 2-wk intervention designed to improve the ability of young and old adults to match a force-time template was associated with changes in the recruitment threshold and the discharge rates of motor units in tibialis anterior.

The third category of mechanisms involves the activation pattern of the population of motor units, which includes both short-term synchronization and common rhythmic modulation of discharge rates. As with the CV for discharge rate, computer simulations have demonstrated that motor-unit synchronization can increase force fluctuations (Yao et al. 2000). The experimental findings with the first dorsal interosseus muscle, however, are mixed. There was a positive association between the amount of motor-unit synchronization and the fluctuations in index finger acceleration during slow anisometric contractions performed by young adults (Semmler et al. 2001), but not between motor-unit synchronization and the fluctuations in index finger force during low-force isometric contractions performed by young and old adults (Semmler et al. 2000). In contrast to the absence of an effect attributed to short-term synchronization during isometric contractions, Halliday et al. (1999) found that the amplitude of physiological tremor was associated with significant coherence in the bandwidths of 1–12 and 15–32 Hz for motor-unit discharge. The frequency-domain correlation in motor-unit discharge is interpreted to represent rhythmic inputs to the motor neurons (Brown 2000; De Luca and Erim 2002; Farmer et al. 1993; Kakuda et al. 1999; Kilner et al. 2002). Thus it does appear that common inputs to motor neurons can contribute to the force fluctuations, at least during low-force contractions.

Comparison of the model and experimental force variability

To distinguish among potential mechanisms, the CVs for force that were obtained with the different models were compared with the experimental measurements across a wide range

of contraction intensities. Two of the models (basic and 20-Hz oscillation) matched the experimental force variability at 6 of the 9 target forces, whereas another 2 models (synchronization and 1-Hz oscillation) were similar at 4 or 5 of the 9 forces. With the exception of the synchronization model, the other 7 models all exhibited a hyperbolic relation between target force and the CV for force, rather than the cubic function with a minimum at about 30% MVC force observed in the experimental measurements. The overall shape of the relation between mean force and CV for force was similar for the synchronization model and the experimental data. The synchronization model, however, showed an initial decline in the magnitude of the CV to a minimum at 15% MVC force compared with the experimental data, which declined to a minimum at 30% MVC force before increasing again. Although several of these models demonstrated relatively constant values for the CV at intermediate target forces (15–30% MVC force), they all failed to reach a plateau of greater values at target forces above 50% MVC.

The results obtained with the synchronization model provided new information on the contribution of discharge rate variability to the fluctuations in force. Previous simulations have demonstrated that physiological differences in the CV for discharge rate (10 vs. 40%) can cause marked differences in the force fluctuations (Enoka et al. 2003; Taylor et al. 2000). Although the CV for discharge rate was approximately twice as large during the current simulations with the synchronization model, the force fluctuations (SD and CV) were similar to those observed with the other models. The lack of a parallel effect of discharge variability in the synchronization and basic models suggests that the presence of motor-unit synchronization may act in some instances to dampen the effect of discharge-rate variability on force fluctuations. Although synchronization augments motor-unit twitches (Taylor et al. 2002), this effect is substantial only for high-threshold motor units whose recruitment contributes the least to the net force (Fuglevand et al. 1993). Nonetheless, the relation between the CV for force and the target force approached a plateau at high target forces with the synchronization model compared with the other models (Fig. 6B), which suggests that motor-unit synchronization likely contributed to the relation observed in the experimental measurements.

Complexity of the model

The study of physiological mechanisms usually requires the construction of a theoretical model of the system to determine the role of factors that influence its function. The theoretical construct can then be implemented in a computational model to identify causal relations between the factors included in the model. Because the model is necessarily more simplistic than the physiological system, it is easier to isolate the variables that are important to the phenomenon of interest. Furthermore, the failures of the model are often as instructive as successes because they indicate areas of the theoretical construct that need to be modified. Accordingly, the current simulations provided a key new insight on the origin of the force fluctuations: the temporal relations between the discharge times of all the motor units in a muscle are crucial to reproduce the patterns of force variability that were observed experimentally. How-

ever, there remain some differences between the experimental data and the model as it is currently implemented.

The simulated coefficients of variation for force had a consistent DC shift relative to the experimental data, especially at low forces. Two features of the model may have been responsible for this difference in the normalized force fluctuations: the linear summation of motor-unit force and the uniform excitation function. Studies conducted on the hindlimb muscles of cats indicate that the force produced by multiple motor units is often not equivalent to the algebraic sum of the forces from the individual motor units (Clamann and Schelhorn 1988; Perreault et al. 2003; Powers and Binder 1991). The degree of nonlinearity in these studies depended on the magnitude of the force that was produced and the type of muscle contraction. It is hypothesized that the nonlinear summation of force depends on the mechanical interactions between the muscle fibers and connective tissue. Because the magnitude and pattern of nonlinearity reported in the literature are variable, forces were assumed to sum linearly in the model. However, if the force produced by a group of motor units is greater than the linear sum of the individual forces, the force produced by the model might underestimate the corresponding experimental values and result in a larger CV for force, as was observed at low forces. Provided this effect is uniform across the population, errors in estimating force amplitude should not influence the variation in force fluctuations with contraction intensity, which depend on the degree of twitch fusion and the timing of motor-unit twitches.

The divergence of the simulated coefficients of variation for force from the experimental data around 15 to 30% MVC may also be influenced by the simplified excitation function of the current motor-unit model. For example, the CV for force for the 20-Hz oscillation model had one of the best fits to the experimental CVs at different force levels and the 1-Hz oscillation model provided a good approximation of the experimental forces in the frequency domain. Thus the variation in force fluctuations may be attributable to rhythmicities in the discharge rate of motor units. Because the individual motor units operate on the steep portion of the force–frequency relation at moderate forces, relatively small changes in instantaneous discharge rate in this region would have a large influence on motor-unit force. Furthermore, all motor units in the model received the same excitatory drive, including the oscillatory drive that was imposed on the discharge frequency with zero phase delay between motor units. However, recordings from the cortex of nonhuman primates indicate that there is variability in the time delay between oscillations (Murthy and Fetz 1996). With asynchronous modulation, fewer motor units would discharge with similar timing, which might reduce the fluctuations in the force signal. To address this possibility, we are currently developing a more realistic model of synaptic activation of the pool of motor neurons (Taylor and Enoka 2002).

Comparison of model and experimental power spectra

As reported previously, both the experimental and simulated forces contained significant power in the frequency spectrum below 2 Hz in the frequency domain (De Luca et al. 1982; Vaillancourt and Newell 2003; Vaillancourt et al. 2002). The low-frequency component observed in the models without

oscillating activation is likely a result of the mechanical characteristics of force production; the one feature of the models that was consistent across conditions was the process of summation of motor-unit twitches to produce whole muscle force. However, the low-frequency component contained more power for the 1-Hz oscillation model compared with that of the other models. Thus the current simulation results indicate that the low-frequency component in the force spectrum is attributable to both a low-frequency modulation of motor neuron discharge and a mechanical component ascribed to the summation of motor unit twitches.

In addition to the low-frequency peak in the power spectra, however, three of the most explanatory models (basic, 1-Hz oscillation, and 20-Hz oscillation) also exhibited secondary peaks at higher frequencies that were not present in the experimental records. Because the secondary peaks corresponded to the mean discharge rates at each target force, the average frequencies increased with the level of excitation and were less distinct in models with greater variability in discharge rate. For example, the secondary peaks in the power spectra broadened but the average frequency remained similar when the CV for discharge rate was doubled (10 to 20%). This effect was less obvious with the synchronization model, presumably because of the greater variability in discharge rate. Despite the relatively large amplitude (10%) of the modulation in excitation for the 20-Hz oscillation model, the most significant secondary peak paralleled the mean discharge rate and not the imposed 20-Hz oscillation. These results suggest that the high-frequency fluctuations often observed in acceleration records (Halliday et al. 1999; McAuley et al. 1997) are probably not attributable to high-frequency modulation of synaptic input to motor neurons.

Although the regression analyses identified statistically significant associations between the fluctuations in force (SD and CV) and spectral characteristics of the simulated and experimental forces, the coefficients of determination were low (average $r^2 = 0.18 \pm 0.10$). Furthermore, the sign of these correlations sometimes differed for the experimental and simulated forces. For example, the low frequencies of the simulated forces, with the exception of the synchronization model, were negatively related to the SD of force, whereas the low frequencies in the experimental force were positively associated with the SD of force. In contrast, the amplitude of the CV for force, in both the experimental and simulated records, increased with power in the low frequencies in the force spectra. These results underscore the inadequacy of any single mechanism for predicting the composite structure of the force signal.

In conclusion, force variability changes nonlinearly across the entire range of excitation levels that impinge on the motor-neuron population. The results of the modeling work suggest that manipulation of recruitment and rate coding alone could not adequately describe the patterns of force fluctuations. The pattern of force variability, however, does appear to rely on the composite activity of the motor-unit population. Alterations in the relative timing of action potentials attributed to different activation patterns reproduced some features of the experimental force signal and patterns of variability. Consequently, the pattern of force fluctuations most likely depends on the interaction of multiple features of motor-unit activity.

DISCLOSURES

This study was supported by Grant AG-09000 from the National Institute on Aging to R. M. Enoka and a National Science Foundation Graduate Research Fellowship awarded to A. M. Taylor.

REFERENCES

- Allen GM, Gandevia SC, and McKenzie DK. Reliability of measurements of muscle strength and voluntary activation using twitch interpolation. *Muscle Nerve* 18: 593–600, 1995.
- Burnett RA, Laidlaw DH, and Enoka RM. Coactivation of the antagonist muscle does not covary with steadiness in old adults. *J Appl Physiol* 89: 61–71, 2000.
- Christou EA, Grossman M, and Carlton LG. Modeling variability of force during isometric contractions of the quadriceps femoris. *J Mot Behav* 34: 67–81, 2002.
- Clamann HP and Schelhorn TB. Nonlinear force addition of newly recruited motor units in the cat hindlimb. *Muscle Nerve* 11: 1079–1089, 1988.
- Day SJ and Hulliger M. Experimental simulation of cat electromyogram: evidence for algebraic summation of motor-unit action-potential trains. *J Neurophysiol* 86: 2144–2158, 2001.
- De Luca CJ, LeFever RS, McCue MP, and Xenakis AP. Control scheme governing concurrently active human motor units during voluntary contractions. *J Physiol* 329: 129–142, 1982.
- Enoka RM, Christou EA, Hunter SK, Kornatz KW, Semmler JG, Taylor AM, and Tracy BL. Mechanisms that contribute to differences in motor performance between young and old adults. *J Electromyogr Kinesiol* 13: 1–12, 2003.
- Enoka RM and Fuglevand AJ. Motor unit physiology: some unresolved issues. *Muscle Nerve* 24: 4–17, 2001.
- Farmer SF. Rhythmicity, synchronization and binding in human and primate motor systems. *J Physiol* 509: 3–14, 1998.
- Fuglevand AJ, Winter DA, and Patla AE. Models of recruitment and rate coding organization in motor-unit pools. *J Neurophysiol* 70: 2470–2488, 1993.
- Halliday DM, Conway BA, Farmer SF, and Rosenberg JR. Load-independent contributions from motor-unit synchronization to human physiological tremor. *J Neurophysiol* 82: 664–675, 1999.
- Jones KE, Hamilton A, and Wolpert DM. The sources of signal-dependent noise during isometric force production. *J Neurophysiol* 88: 1533–1544, 2002.
- Keen DA, Yue GH, and Enoka RM. Training-related enhancement in the control of motor output in elderly humans. *J Appl Physiol* 77: 2648–2658, 1994.
- Kornatz KW, Christou EA, and Enoka RM. Steadiness training reduces the variability of motor unit discharge rate in isometric and anisometric contractions performed by old adults. *Soc Neurosci Abstr* 28: 665.10, 2002.
- Laidlaw DH, Bilodeau M, and Enoka RM. Steadiness is reduced and motor unit discharge is more variable in old adults. *Muscle Nerve* 23: 600–612, 2000.
- Laidlaw DH, Kornatz KW, Keen DA, Suzuki S, and Enoka RM. Strength training improves the steadiness of slow lengthening contractions performed by old adults. *J Appl Physiol* 87: 1786–1795, 1999.
- Macefield VG, Fuglevand AJ, and Bigland-Ritchie B. Contractile properties of single motor units in human toe extensors assessed by intraneural motor axon stimulation. *J Neurophysiol* 75: 2509–2519, 1996.
- McAuley JH, Rothwell JC, and Marsden CD. Frequency peaks of tremor, muscle vibration and electromyographic activity at 10 Hz, 20 Hz and 40 Hz during human finger muscle contraction may reflect rhythmicities of central neural firing. *Exp Brain Res* 114: 525–541, 1997.
- Murthy VN and Fetz EE. Oscillatory activity in sensorimotor cortex of awake monkeys: synchronization of local field potentials and relation to behavior. *J Neurophysiol* 76: 3949–3967, 1996.
- Patten C and Kamen G. Adaptations in motor unit discharge activity with force control training in young and older human adults. *Eur J Appl Physiol* 83: 128–143, 2000.
- Perreault EJ, Day SJ, Hulliger M, Heckman CJ, and Sandercock TG. Summation of forces from multiple motor units in the cat soleus muscle. *J Neurophysiol* 89: 738–744, 2003.
- Person RS and Kudina LP. Discharge frequency and discharge pattern of human motor units during voluntary contraction of muscle. *Electroenceph Clin Neurophysiol* 32: 471–483, 1972.

- Powers RK and Binder MD.** Summation of motor unit tensions in the tibialis anterior muscle of the cat under isometric and nonisometric conditions. *J Neurophysiol* 66: 1838–1846, 1991.
- Sears TA and Stagg D.** Short-term synchronization of intercostal motoneurone activity. *J Physiol* 263: 357–381, 1976.
- Semmler JG.** Motor unit synchronization and neuromuscular performance. *Exerc Sport Sci Rev* 30: 8–14, 2002.
- Semmler JG, Kornatz KW, Kern DS, and Enoka RM.** Motor unit synchronization reduces the steadiness of anisometric contractions by a hand muscle. *Soc Neurosci Abstr* 27: 168.3, 2001.
- Semmler JG, Steege JW, Kornatz KW, and Enoka RM.** Motor-unit synchronization is not responsible for larger motor-unit forces in old adults. *J Neurophysiol* 84: 358–366, 2000.
- Slifkin AB and Newell KM.** Noise, information transmission, and force variability. *J Exp Psychol* 25: 837–851, 1999.
- Slifkin AB, Vaillancourt DE, and Newell KM.** Intermittency in the control of continuous force production. *J Neurophysiol* 84: 1708–1718, 2000.
- Taylor AM and Enoka RM.** Model motor neurons with active dendrites require more input synchrony than passive models for the same level of motor unit synchrony. *Soc Neurosci Abstr* 28: 856.11, 2002.
- Taylor AM, Steege JW, and Enoka RM.** Increased variability of motor unit discharge rate decreases the steadiness of simulated isometric contractions (Abstract). *Physiologist* 43: 321, 2000.
- Taylor AM, Steege JW, and Enoka RM.** Motor-unit synchronization alters spike-triggered average force in simulated contractions. *J Neurophysiol* 88: 265–276, 2002.
- Thomas CK, Bigland-Ritchie B, and Johansson RS.** Force-frequency relationships of human thenar motor units. *J Neurophysiol* 65: 1509–1516, 1991.
- Vaillancourt DE, Larsson L, and Newell KM.** Time-dependent structure in the discharge rate of human motor units. *Clin Neurophysiol* 113: 1325–1338, 2002.
- Vaillancourt DE and Newell KM.** Aging and the time and frequency structure of force output variability. *J Appl Physiol* 94: 903–912, 2003.
- Yao W, Fuglevand AJ, and Enoka RM.** Motor-unit synchronization increases EMG amplitude and decreases force steadiness of simulated contractions. *J Neurophysiol* 83: 441–452, 2000.
- Zijdewind I, Zwarts MJ, and Kernell D.** Fatigue-associated changes in the electromyogram of the human first dorsal interosseous muscle. *Muscle Nerve* 22: 1432–1436, 1999.